



## THE REMEDIATION POTENTIAL OF BIOCHAR DERIVED FROM *Morus rubra* LINN. BARK

(Potensi Pemulihan oleh Terbitan Arang Bio dari Kulit Kayu *Morus rubra* Linn.)

Judith Clarisse Jose<sup>1</sup>, Mark Nathaniel Dolina<sup>2</sup>, Maria Carmen Tan<sup>2\*</sup>

<sup>1</sup>Biology Department

<sup>2</sup>Chemistry Department

De La Salle University, 2401 Taft Avenue, Manila 0922, Philippines

\*Corresponding author: maria.carmen.tan@dlsu.edu.ph

Received: 15 December 2020; Accepted: 27 March 2021; Published: 25 April 2021

### Abstract

*Morus rubra* L., commonly known as red mulberry, contains a myriad of phytochemical compounds. Mulberry plants have been previously studied for their potential in the phytoremediation process of potentially toxic elements (PTEs). In this study, biochars of red mulberry bark were produced by hydrothermal carbonization using a hydrothermal autoclave reactor (HAR) with PTFE liner and a Parr oxygen combustion vessel (POCV). These biochars were chemically characterized and their remediation potential were also investigated. Solvent extraction using dichloromethane was performed on the bark and biochars derived therefrom and the subsequent samples were evaluated using gas chromatography – electron ionization– mass spectrometry (GC–EI–MS). Scanning electron microscopy (SEM) provided the exterior characterization of these biochars, together with the dried red mulberry bark. Compositional analyses were determined by an energy dispersive X-ray spectrometer (EDX) and a Fourier transform infrared spectrometer (FT-IR). The biochar's remediation potential of toxic heavy metals was discerned by atomic absorption spectroscopy. Phytochemical analyses revealed the constituents of red mulberry bark which included phytosterol, triterpenes, and triterpenoids, whereas, biochars contained esters, alkanes, alkenes, alkaloids, diene, and fatty alcohol. Comparing the two carbonization processes, the Parr oxygen combustion vessel (POCV) was able to carbonize red mulberry bark more than the hydrothermal autoclave reactor (HAR) with PTFE liner, as observed in their GC-EI-MS and SEM profiles. Elemental analysis showed high percentages of oxygen and carbon in red mulberry bark due to the presence of carbohydrates. Both biochar products effectively absorbed lead (Pb) by almost 60% and minimally absorbed cadmium (Cd) and iron (Fe) in the heavy metal solution. Copper (Cu) and chromium (Cr) were not remediated from the heavy metal solution by both biochar samples.

**Keywords:** *Morus rubra* L., gas chromatography-electron ionization-mass spectrometry, scanning electron microscopy, Fourier transform infrared spectroscopy, energy dispersive X-ray analysis

### Abstrak

*Morus rubra* L. umum dikenali sebagai mulberi merah, kaya dengan kandungan sebatian fitokimia. Pokok mulberi pada kajian terdahulu melihat potensinya dalam proses fitoremediasi terhadap unsur toksik (PTEs). Dalam kajian ini, arang bio dari kulit kayu mulberi merah telah dihasilkan melalui pengkarbonan hidrotermal menggunakan reaktor autoklaf hidrotermal (HAR) dengan liner PTFE dan vesel pembakaran oksigen Parr (POCV). Arang bio yang terhasil dicirikan secara kimia dan potensi pemulihannya turut dikaji. Pengekstrakan pelarut diklorometana digunakan terhadap kulit kayu dan terbitan arang bio dan diikuti analisis menggunakan spektrometri jisim-pengionan elektron-kromatografi gas (GC-EI-MS). Mikroskopi imbasan elektron (SEM) menjelaskan pencirian

luar arang bio bersama kayu kulit mulberi merah yang telah dikeringkan. Analisis komposisi telah ditentukan melalui spektrometer sinar-X serakan tenaga (EDX) dan spektrometer inframerah transformasi Fourier (FT-IR). Potensi pemulihan arang bio terhadap ketoksikan logam berat telah dianalisa menggunakan spektroskopi serapan atom. Analisis fitokimia menjelaskan jujukan kimia bagi kulit kayu mulberi merah termasuklah fitosterol, triterpene, dan triterpenoid, manakala arang bio mengandungi ester, alkana, alkena, alkaloid, diena dan lemak alkohol. Perbandingan dua proses pengkarbonan vesel pembakaran oksigen Parr (POCV) mampu menghasilkan karbon yang lebih tinggi kandungannya berbanding reaktor autoklaf hidrotermal (HAR) dengan liner PTFE, diperhatikan dalam profil GC-EI-MS dan SEM. Analisis unsur telah menunjukkan peratusan tinggi kehadiran oksigen dan karbon di dalam kulit kayu mulberi merah disebabkan oleh kandungan karbohidrat. Produk arang bio berkesan menyerap plumbun (Pb) sehingga 60% dan serapan minima bagi kadmium (Cd) dan ferum (Fe) di dalam larutan logam berat. Kuprum (Cu) dan kromium (Cr) tidak dapat dipulihkan dari larutan logam berat oleh kedua-dua sampel arang bio.

**Keywords:** *Morus rubra* L., spektrometri jisim-pengionan elektron-kromatografi gas, mikroskopi imbasan elektron, spektrometer inframerah transformasi Fourier, spektrometer sinar-X serakan tenaga

### Introduction

The notable attention that is being given to timber-derived resources as a substitute of activated carbon for commercial adsorbent purposes is largely due to its efficient loading function, high availability, and low production expenditure [1]. Biochar is a high-carbon solid residue formed from pyrolysis processes. Biochar efficiency is largely dependent on the type of feedstock used, and the conditions of pyrolysis [2]. Apart from remediation of soil that has been contaminated by potentially toxic elements (PTEs), biochar can also remove other pollutants like organic substances, improve soil quality for agricultural productivity, and reduce greenhouse gases [3]. The macroporosity in granular wood-based hydrochar has been found to result in high sorption capacities [1].

*Morus rubra* L. (MR) is known as the scarlet mulberry which is indigenous to Eastern as well as Central North America. Additionally, MR is regarded as an endangered tree species in some parts of the United States and Canada, prompting its conservation [4]. MR has been established to be part of the Moraceae family along with the *Morus* genus, MR is classified as a perennial, deciduous, and woody plant [5]. The foliage of MR has been observed to be morphologically similar to black mulberry greenery (*Morus nigra*), although MR tends to possess thicker, lobed, and larger leaves [4]. *Morus* berries have also been in traditional medicine as a laxative, dewormer, emetic, anthelmintic, hypoglycemic agent, and to treat dysentery [6].

Numerous phytochemical compounds with antidiabetic properties such as flavonoids, alkaloids, triterpenes, saponins, sterols, glycosides, and phenolics have been found in the different parts as per *Morus* species [7]. It is the presence of these phytochemical compounds that give the mulberry plant its reported antidiabetic, anticorpulence, anti-inflammatory, carcinopreventive, bactericidal, free radical scavenging, prophylactic for viruses, cytoprotectant and neuroprotectant capacities [8]. Comparative studies among different mulberry species have been done to investigate possible differences in bioactivities found in their leaves, fruit, and bark. In one study, leaves and bark samples from *Morus alba* and MR were collected to evaluate their antioxidant and antibacterial activity. The results showed all extracts displaying significant antioxidant activity, with aqueous extracts from stem bark exhibiting greater antioxidant activity. The highest IC<sub>50</sub> value reported among the samples was of MR, at 4.78 mg/ml. On the other hand, hydromethanolic extracts were found to have higher antimicrobial activity than aqueous extracts [9]. Another study involved aqueous MR leaf extracts being administered to rats, and it was found that at least 400 mg/kg of the MR extract were able to control hyperglycemia and dyslipidemia. Its exceptional antioxidant properties were propositioned to help ease complications arising from diabetes [7]. The cytotoxic effects of DMSO extracts of MR trials on homo sapiens colon adenocarcinoma (WiDr) were also investigated. MR extracts were found to exhibit moderate selective toxicity on colon cancer cells and significantly repress telomerase. The IC<sub>50</sub> value was found to be 297.4 +/- 9.6 µg/mL [10]

Amino acid content analysis of black, white, and red mulberry leaves found fifteen different aminoalkanoic acids, namely glutamic acid, glycine, methionine, and tyrosine, with superior concentrations of amino acid groups detected in *M. alba* foliage. Extractions using 40% ethanol as the solvent yielded different micronutrients (phenolic acids) such as gallic acid, caffeic acid, chlorogenic acid, as well as tannin acid. Chlorogenic acid generated a quantitative content of 0.14% and rutin having a value of 0.058% [11]. Fatty acid analysis of *M. alba*, MR, and *M. nigra* revealed varying concentrations of unsaturated fatty acids which was mostly made up of linoleic acid, palmitic acid, and oleic acid [6]. Statistically significant differences in total anthocyanin content have been found between *M. nigra* and MR. Black mulberry berries were reported to have higher anthocyanin content (674-787 Cy 3-glu  $\mu\text{g/g}$ ) compared to the content found in red mulberry samples (81-132 Cy 3-glu  $\mu\text{g/g}$ ) [12]. Red mulberry and black mulberry have been noted for their high nutritional value which is largely attributed to their mineral content, though MR has been shown to have a higher Ca content than *M. nigra*, *M. nigra* has less Mg and K in its plant matrix. Moreover, *Morus* species were distinguished to have noteworthy mineral content which was higher than that of other cultivated and harvested fruits [12].

Hitherto, studies have only been limited to the absorption phytoremediation potential of mulberry plants. *Morus* species plants are known for their notable characteristics of swift development of plant growth, rapid proliferation, healthy leaves, and an extensive vascular network which render them appropriate for mitigation of polluted soils [13] especially for cadmium (Cd) and zinc (Zn) phytoextraction [14]. Only a few studies have been done on the remediation potential of its biochar. One study found that biochar derived from *M. alba* was found to have significantly removed Pb from solution, which was attributed to the biochar's chemical properties, namely the presence of organic functional groups (which are rich in electronegative groups), which can act as potential sequestrants [15]. However, the remediation potential of biochar derived from red mulberry bark has yet to be studied. After extensive literature search, the authors presuppose that this work is unique in its endeavor in the

characterization and the investigation of the remediation potential of the biochar produced from the dried bark of the red mulberry species.

## Materials and Methods

### Materials

*M. rubra* bark was collected from Abucay, Bataan, Philippines (14.7128° N, 120.4934° E) on well cultivated arable land. The plant identity was substantiated and authenticated by the Bureau of Plant Industry (BPI) in Malate, Manila, National Capitol Region, Philippines.

### Sample preparation

Dried MR bark was cut and ground into finer pieces. The crude extract was prepared by incubating 100 mg of dried red mulberry bark in dichloromethane (DCM) for 3 hours. The extract was filtered using Whatman filter paper No. 1 (11  $\mu\text{m}$  pore size) and dried over nitrogen gas. The accumulated dried extract (1.3 mg) was diluted in DCM before filtering into a vial using a 0.45  $\mu\text{m}$  syringe filter with a final volume of 1 mL. The sample was analyzed and characterized using gas chromatography – electron ionization – mass spectrometry (GC-EI-MS).

### Hydrothermal carbonization of red mulberry bark

Hydrothermal carbonization (HTC) of dried MR bark was done using a hydrothermal autoclave reactor (HAR) with PTFE liner and a Parr oxygen combustion vessel (POCV). One gram of the outer covering of the MR plant was placed in both HAR and POCV, and both were heated using a furnace at 180 °C for 4 hours, increased at 260 °C for 120 minutes, and at 400 °C for 120 minutes. The temperature was increased until the samples were carbonized. The resulting biochar, a product of HTC obtained from both HAR and POCV, was prepared for GC – EI – MS analyses. One hundred milligrams (100 mg) of each biochar from HAR and POCV were incubated in DCM for 3 hours. The samples were filtered into a beaker by means of a 0.45  $\mu\text{m}$  syringe membrane and were dried over nitrogen gas. The dried samples (1.4 mg for HAR and 1.2 mg for POCV) were concentrated over nitrogen gas and diluted in 1 mL DCM. Each subsequent eluate was then

prefiltered using a 0.45  $\mu\text{m}$  membrane, with a total final volume of 1 mL in each vial (1.5 capacity vial).

#### **Gas chromatography - electron ionization - mass spectrometry**

All samples obtained from DCM extraction of dried red mulberry bark and hydrothermal carbonization of dried MR bark using HAR and POCV at 400 °C were analyzed using an Agilent gas chromatograph in tandem with a mass spectrometer (7890B) with a HP-5ms (5%-phenyl)-methylpolysiloxane Ultra Inert column (30 m x 250 mm x 0.25 mm). Ultrapure helium gas served as the mobile phase (1 mL/min), maintained pressure at 8.2 psi, rate of 36.62 cm/s, and holdup period of 1.37 minutes. The injection inlet (split less) was maintained at 250 °C, with a pressure of 8.2 psi, a flow rate of 24 mL/min, and a septum purge stream velocity of 3 mL/min. The temperature gradient was initially set at 70 °C after which the temperature was incrementally augmented to 2 °C/min to reach 135 °C for 10 minutes. Another temperature ramp was programmed to raise the temperature to 220 °C at 4 °C/min and was held at this temperature for 10 minutes. The final temperature ramp gradually raised to 270 °C at 3.5 °C/min and was held at 37 minutes. The compounds were identified via the National Institute of Standards and Technology (NIST) Archive 2.0. The computation of the % peak area average was derived from the subsequent total ion chromatograms (TIC). Identification was verified by the assessment of the individual constituents based on their order of elution with their relative retention indices on a gas chromatography column (mid-polar). Calculations of retention indices for all the compounds were evaluated using a standard consisting of multiple *n*-alkanes. All tests were performed in triplicates.

#### **Scanning electron microscopy**

A JSM 5310 Scanning Microscope (JEOL, Japan) was used to examine the morphology of the dried MR bark and biochar samples. This instrument uses a focused beam of electrons to scan the surface of the samples. A small amount of each sample was mounted in a metal stub using a conductive carbon adhesive tape and all samples were coated with gold ions for 65 seconds using JFC-1200 Fine Coater (JEOL, Japan). Analyses were

done using SemAfore V.5.2 to analyze the produced image.

#### **Energy dispersive X-ray analysis**

An AMETEK-EDAX Z2e Analyzer was used to collect and analyze the energy dispersive spectroscopy (EDS) data and compositional characterization of the dried MR bark. The EDAX system which is attached to a JSM 5310 Scanning Microscope wherein the imaging ability of SEM identifies the specimen to be analyzed by EDAX. Analyses were done using EDAX APEX™ Review software.

#### **Fourier transform infrared spectroscopy**

A Thermo Scientific Nicolet 6700 FT-IR (Thermo Fisher Scientific, USA) with a DTGS potassium bromide detector (KBr), Csl beamsplitter, and transmission accessory were utilized for the characterization of the samples. Analytical grade KBr was employed to collect the background. Each sample was scanned 16 times from 400-4000  $\text{cm}^{-1}$  with a spectral resolution of 4  $\text{cm}^{-1}$ . Omnic Spectra software 8.0.342 (Thermo Fisher Scientific, USA) was used to analyze the data.

#### **Atomic absorption spectroscopy**

The AA-6300 Atomic Absorption Spectrophotometer, operated with an air-acetylene flame, was utilized for the detection of absorbance of heavy metals of dried MR bark and biochar samples. Copper, iron, lead, cadmium, and chromium were the heavy metals used to create a stock solution of 10 ppm. Working solutions were also prepared with final dilutions of 10 ppm, 5 ppm, 1 ppm, and 0.5 ppm. Three milligrams of each sample were placed in a plastic container and were incubated in 25 mL of different concentrations of working solutions of heavy metals for 72 hours at room temperature. Each trial was then prefiltered using Whatman filter paper No. 1 (11  $\mu\text{m}$  pore size) to remove particulate matter. Standard concentrations of 10 ppm, 5 ppm, 1 ppm, 0.5 ppm, and 0.25 ppm were used for the analyses. Measurement of absorbances were set at the following wavelengths: 324.8 nm for copper [Cu], 248.3 nm for iron [Fe], 283.3 nm for lead [Pb], 228.8 nm for cadmium [Cd], and 357.9 nm for chromium [Cr]. All tests were performed in triplicates.

## Results and Discussion

### GC-MS analyses of dried red mulberry bark and biochar samples

Dried red mulberry bark was extracted using dichloromethane as the extracting solvent. GC-EI-MS identified six eluents from the crude extract. The constituents are enumerated in Table 1 and presented in Figure 1A based on their elution succession using the HP-5ms column. Characterization of the constituents was verified using their retention index based on the NIST Archive 2.0. The extract was mainly composed of triterpenes and phytosterols:  $\alpha$ -amyirin (8.56%), lanosterol (2.61%) and  $\gamma$ -sitosterol (4.11%).

$\alpha$ -Amyirin is a pentacyclic triterpene found to be synthesized by several cultivars of plants. This is known to be usually found with its isomer  $\beta$ -amyirin in plant extracts [16]. These triterpenes have been stated to cover a wide spectrum of biological activities. Reported bioactivities involved anti-hyperglycemic [17], antimicrobial [18], and anti-inflammatory properties [19], among others. They are also known to have weak anti-cancer activity, but newly synthesized derivatives of the compounds improved the anticancer activity of  $\alpha$ ,  $\beta$ -amyirin [20]. Contrastingly,  $\alpha$ -amyirin was shown to stimulate the proliferation of human keratinocytes by up to 18% [16].

Lanosterol was also observed to be present in the extract. It is a tetracyclic triterpenoid from which all steroids are derived [21]. It has been reported that lanosterol could be used as an alternative treatment in human cataracts. The study reported that lanosterol treatment significantly decreased the protein aggregates of various cataract-causing mutant crystallins and could reduce cataract severity [22]. However, another study had shown contradicting results wherein both lanosterol and 25-hydroxycholesterol were found to be unable to counteract lenticular opacities or avert advancements of cataracts [23]. Furthermore, age-related cataractous nuclei also showed progression and no changes even when under treatment with lanosterol for 6 days [24].

Another compound found from the extract is  $\gamma$ -sitosterol. It is a phytosterol that has the potential to be employed as an antidiabetic agent [25].  $\gamma$ -Sitosterol,

purified and separated from *Strobilanthes crispus*, was also tested for its cytotoxicity on several cancer cell lines revealing IC<sub>50</sub> values of 8.3, 21.8, and 28.8  $\mu$ g/mL for Caco-2, HepG2, and MCF-7 cell lines, correspondingly.  $\gamma$ -Sitosterol also suppressed *c-myc* gene, a cancer-causing gene, and induced apoptosis in Caco-2, HepG2 cell lines [26].

Meanwhile, six volatile constituents were identified from the biochar extract produced from HAR (Table 2). The extract was mostly composed of triterpenes, diene, and ester.  $\beta$ -amyirin (31.35%) had the highest peak area, followed by octadecane, 3-ethyl-5-(2-ethylbutyl)-(18.56%), and a-neooleana-3(5),12-diene (17.03%). Other notable compounds like 10-octadecenoic acid, methyl ester (14.83%), olean-13(18)-ene (13.87%) and 4,4,6a,6b,8a,11,11,14b-octamethyl-1,4,4a,5,6,6a,6b,7,8,8a,9,10,11,12,12a,14,14a,14b-octadecahydro-2H-picen-3-one (10.03%) were also identified. Figure 1B presents the mass spectrum of the analyzed biochar obtained from HAR.

$\beta$ -amyirin, which is the major peak in the HAR extract, is a pentacyclic triterpenoid. Pentacyclic triterpenes are acknowledged to be beneficial in metabolic disorders. A mixture of pentacyclic triterpenes  $\alpha$ , $\beta$ -amyirin was investigated and revealed an antihyperglycemic and hypolipidemic effect in mice.  $\alpha$ ,  $\beta$ -Amyirin considerably reduced streptozotocin –stimulated augmentations in blood sugar, cholesterol levels, and triacylglycerols at 10, 30, and 100 mg/kg. However, the mixture did not reduce normal blood sugar levels but exhibited hypolipidemic effects at 100 mg/kg [17]. Most of the components present in the extract were also triterpenes including olean-13(18)-ene and 4,4,6a,6b,8a,11,11,14b-octamethyl-1,4,4a,5,6,6a,6b,7,8,8a,9,10,11,12,12a,14,14a,14b-octadeca hydro-2H-picen-3-one, which is also known as  $\beta$ -amyrone. Both mentioned triterpenes are  $\beta$ -amyirin derivatives [27, 28].

The biochar obtained from POCV was also analyzed via GC-EI-MS. A total of nine (9) eluents were observed and identified as listed in Table 3. The major peaks in the extract were composed of mostly esters, alkaloids, and fatty alcohol. 10-octadecenoic acid, methyl ester

had the highest peak area of 31.89% among all eluents, followed by 1,3-benzenedicarboxylic acid, bis(2-ethylhexyl) ester (21.01%). 10-Octadecanoic acid, methyl ester was reported to have antibacterial, antifungal, and antioxidant properties, and was found to decrease blood cholesterol [29].

It is worth mentioning that although GC-MS analysis of biochar from POCV (Figure 1c) identified more peaks (9 peaks) from the extract compared with the extract of biochar obtained from HAR (6 peaks), there is a great difference in their abundance numbers. The highest peak from HAR analysis had an abundance of 2 800 000 compared to the highest peak from POCV analysis which had only an abundance of 650 000. This could imply that POCV had carbonized the dried red mulberry bark more than HAR. The retention time (RT) of the major peaks from POCV coincided with the RT of the minor peaks from the chromatogram of HAR analyses.

#### SEM analyses

The surface morphology of dried MR bark and biochar products of HAR and POCV were analyzed using SEM. Scans of dried red mulberry bark seemingly showed square to rectangular patterns with dimensions of  $10.29 \pm 3.46 \times 14.13 \pm 1.85 \mu\text{m}$  (mean  $\pm$  standard deviation) as shown in Figure 2 (a-b). Flakes and small particles measuring  $3.10 \pm 1.25 \mu\text{m}$  can also be observed. At 2000x magnification (Figure 2a) other regions of dried red mulberry bark appeared similar to rounded microparticles measuring  $2.30 \pm 0.67 \mu\text{m}$  which was prominent at the surface of the sample.

SEM photographs of biochars produced from HAR (Figure 2, c-d) and POCV (Figure 2, e-f) revealed a more distinct patterns similar to cork wood. Porous channels measuring  $7.77 \pm 0.65 \mu\text{m}$  were visible at 2000x magnification (Figure 2d) of biochar produced by HAR. However, it can be noticed that the biochar product of POCV did not display distinct geometrical patterns as compared to HAR with pores measuring  $5.42 \pm 1.08 \mu\text{m}$  (Figure 2e). This could also be an indication that POCV had a greater carbonization effect on the dried red mulberry bark than using HAR upon pyrolysis.

The patterns of both biochars from HAR and POCV SEM images were similar to the pattern of cork derived from the outer covering of the tree *Quercus suber* L., which was described as honeycomb-shaped cells. The cork of *Quercus suber* L. was used as a natural sustainable template to synthesize a highly porous ZnO-based biomorphic materials. The cork template was infiltrated with an aerosol to prepare ZnO with zinc acetate and nitrate used as precursors. Heating the infiltrated experiments at 350 °C maintained the honeycomb-shaped cells of the original structure of cork template. This methodology produced a graphite-comprising material that had dual physical adsorption and photocatalytic potential, which made it suitable for environmental remediation [30]. In this research, the dried red mulberry bark was heated multiple times with temperatures ranging from 180 °C to 400 °C. The SEM images of both biochars shown in Figure 2 (C–F) were the result of the pyrolysis of the bark at 400 °C. The biochar of HAR produced a well-defined cork structure compared to the biochar produced by POCV. However, the observance of the presence of porosity in both biochars could indicate that both carbonization processes were suitable for the production of environmental remediation materials.

#### EDX analysis

The elemental composition of dried red mulberry bark was investigated using the AMETEK-EDAX Z2e Analyzer. The EDAX APEXTM Review software revealed six elements present in the bark including oxygen (O) 52.76%, carbon (C) 33.82%, calcium (Ca) 7.92%, potassium (K) 3.21%, magnesium (Mg) 1.24%, and copper (Cu) 1.05%. Fresh sample of *M. alba* fruit also revealed similar elemental compositions with high potassium following carbon and oxygen content [31]. The scanning image and elemental analysis of MR is shown in Figure 3.

Carbon and oxygen are integral elements that can be found in plants, particularly in the form of carbon dioxide, which plays a significant role in the process of photosynthesis together with water to form simple sugars or carbohydrates [32]. These carbohydrates, such as cellulose, hemicelluloses, and polysaccharides covalently bonded to lignin, whether for structural or

storage purposes, are crucial to the development of the plant. The bark or outer covering is most made up of starch, a non-soluble sugar, although other plant species have been found to store other soluble plant sugars as well, such as glucose and fructose [33]. Calcium, in the form of  $\text{Ca}^{2+}$  ions, is an element collected by plants through the soil, and commonly transported through the xylem for the purpose of influencing plant enzymes such as phospholipase and other proteins which aid in plant growth [34]. The recommended dietary allowance for calcium can vary from 1,000 to 1,300 mg/day for adults [35]. Potassium is also essential to both cellular and reaction mechanisms in human physiology. In fact, potassium and sodium are the primary electrolytes that control the water equilibrium and the acid-base equilibrium in bodily homeostasis [36]. Adequate intakes (AIs) for potassium are within the range of 2,600 mg/day for adult females and 3,400 mg/day for adult males [37].

Magnesium, an essential element in biochemical functions of several metabolic processes, is used in therapeutics of various commonplace illnesses specifically migraines, metabolic disorders, diabetes, hyperlipidemia, asthma, premenstrual syndrome, preeclampsia, and differing cardiac arrhythmias [38]. The current recommended dietary allowance (RDA) for magnesium is 320 mg/day for adult females and 420 mg/day for adult males [39]. On the other hand, copper is considered a necessary element but has been found to be detrimental if it accumulates in living systems. The tolerable upper intake level for copper sourced from food and supplements is at 10,000 mcg for individuals older than 19 years old [40]. The WHO (World Health Organization) advocates the consumption of 30  $\mu\text{g}$  per kg of body weight per day of copper to ensure sufficient health requirements. Cardiovascular integrity, lung elasticity, neovascularization, neuroendocrine function, and iron metabolism is also dependent on the presence of copper. Conversely, high intake of copper may induce toxicity and eventual onset of disease [41].

#### FTIR analyses

The dried red mulberry bark and biochars produced from HAR and POCV were characterized by FTIR. Figure 4 presents the FTIR patterns of all the samples.

The peak patterns of the three samples were almost like one another. The mid infrared (IR) absorptions, with a wavenumber range of 4,000 to 400  $\text{cm}^{-1}$  (wavelengths 2.5 to 25  $\mu\text{m}$ ), of the dried red mulberry bark is represented in Table 4. The peak obtained at 3416.65  $\text{cm}^{-1}$  has been ascribed to the stretching of O – H bands implicating the presence of an alcohol. The peaks within at 3000 – 2840  $\text{cm}^{-1}$  has been corresponded to C – H stretching of an alkane, whereas the peak at 1629.04  $\text{cm}^{-1}$  has been correlated to the stretching of C = C bands of a conjugated alkene. Meanwhile, the peak obtained at 11427.61  $\text{cm}^{-1}$  corresponded to the O – H bending from a carboxylic acid. Peaks within 1390 – 1310  $\text{cm}^{-1}$  has been associated with the presence of phenols because of the O – H bending. The presence of an alkyl aryl ether has been correlated to the C – O stretching of peak obtained at 1246.45  $\text{cm}^{-1}$ . The peak obtained at 1060.13  $\text{cm}^{-1}$  corresponded to the stretching of C – O bands of a primary alcohol.

Similar observations were also exhibited in the FTIR spectrum patterns of the biochar produced from HAR (Table 5). The peak acquired at 3430.31  $\text{cm}^{-1}$  has been linked to the O – H stretching of an alcohol. Peaks obtained within 3000 – 2840  $\text{cm}^{-1}$  can be attributed to the C – H stretching of an alkane. A cyclic alkene may perhaps be present due to the C = C stretching of the peak seen at 1555.05  $\text{cm}^{-1}$ . Peaks obtained at 1445.30  $\text{cm}^{-1}$  can be attributed to the bending of O – H bands from a carboxylic acid, while the peaks shown within 1390 – 1310  $\text{cm}^{-1}$  may possibly correspond to O – H bending of phenol compounds. The peak at 1087.67  $\text{cm}^{-1}$  has been connected to the stretching of C – O bands of an aliphatic ether.

Occurrences of C – H stretching and methylene bending in the FTIR analyses revealed the possible presence of aliphatic and olefinic hydrocarbons in the dried red mulberry bark and biochars produced from HAR and POCV [42] as well as aromatic breakdown products associated with pyrolysis [43].

Table 6 presents the FTIR correlations because of the biochar generated from POCV. The peaks obtained are most likely to be attributed to the presence of alcohols by the stretching of O – H bands and C – O bands. The

peak at 2920.87  $\text{cm}^{-1}$  corresponded to the C – H stretching of an alkane, while the peak at 1625.45  $\text{cm}^{-1}$  was correlated to the C = C stretching from a conjugated alkene. The peak ascribed at 1427.71  $\text{cm}^{-1}$  was assigned to the bending of O – H bands from a carboxylic acid.

The peak at 1380.92  $\text{cm}^{-1}$  was attributed to the C – H bending representing an alkane.

Table 1. Volatile constituents of dichloromethane crude extract of dried red mulberry bark

Compound	RT (min)	RI <sup>(a)</sup>	% Peak Area	Functionality
1 $\gamma$ -sitosterol	100.56	3487	4.11	Phytosterol
2 lanosterol	102.51	3426	2.61	Triterpenoid
3 $\alpha$ -amyrin	103.98	3453	8.56	Triterpene
4 12-oleanen-3-yl acetate, (3 $\alpha$ )-	108.35	3448	15.58	Triterpene
5 lanosta-8,24-dien-3-ol, acetate, (3 $\beta$ )-	109.46	3470	8.44	Triterpenoid
6 12-oleanen-3-yl acetate, (3 $\alpha$ )-	111.59	3466	58.70	Triterpene

<sup>(a)</sup>Retention Index (HP 5ms column)

Table 2. Volatile constituents of biochar obtained using HAR

Compound	RT (min)	RI <sup>(a)</sup>	% Peak Area	Functionality
1 10-octadecenoic acid, methyl ester	60.47	2101	14.83	Ester
2 octadecane, 3-ethyl-5-(2-ethylbutyl)-	83.03	2899	18.56	Alkane
3 a-neooleana-3(5),12-diene	85.44	2892	17.03	Diene
4 $\beta$ -amyrin	89.53	3064	31.35	Triterpene
5 olean-13(18)-ene	90.37	3099	13.87	Triterpene
6 1,4,4a,5,6,6a,6b,7,8,8a,9,10,11,12,12a,14,14a,14b-octadecahydro-2H-picen-3-one	102.45	3425	10.03	Triterpene

<sup>(a)</sup>Retention Index (HP 5ms column)



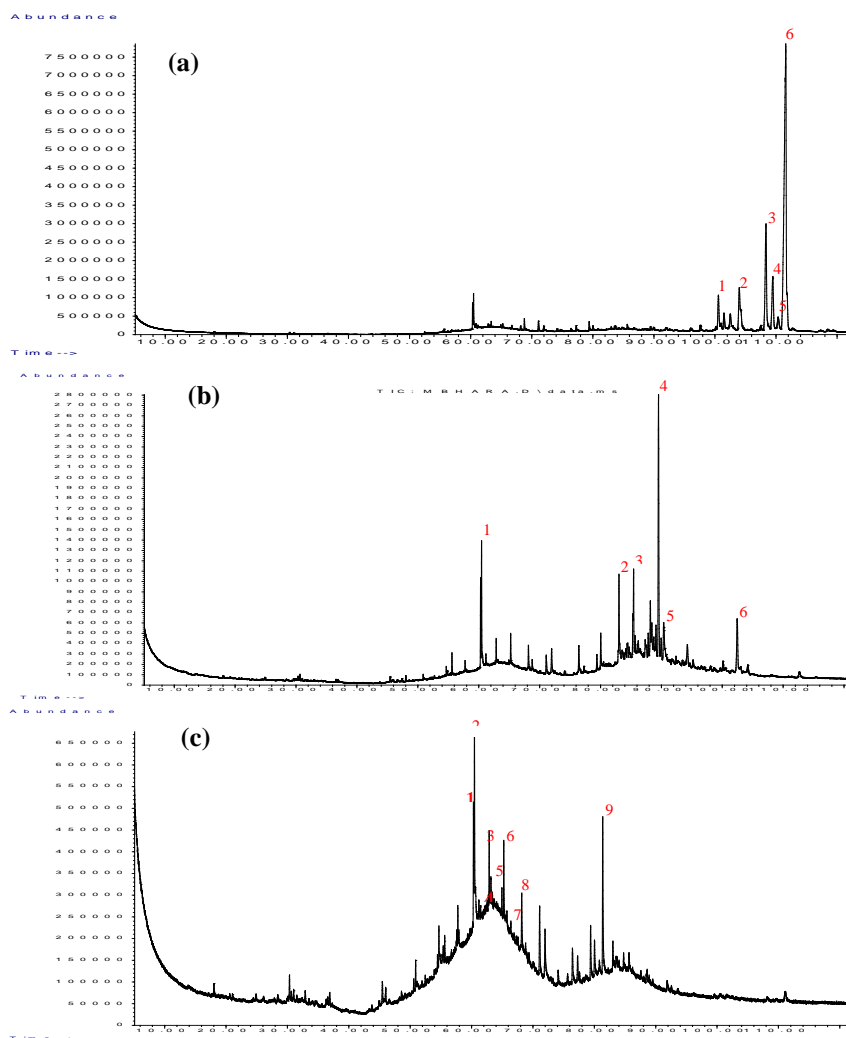


Figure 1. Total ion chromatograms of (A) dried MR bark, (B) hydrochar from HAR, and (C) hydrochar from POCV

Table 3. Volatile constituents of biochar obtained using POCV

Compound	RT (min)	RI <sup>(a)</sup>	% Peak Area	Functionality
1 8,11-octadecadienoic acid, methyl ester	60.32	2095	12.56	Ester
2 10-octadecenoic acid, methyl ester	60.48	2101	31.89	Ester
3 ethyl iso-allocholate	60.65	2108	9.58	Alkaloid
4 2,7-Diphenyl-1,6-dioxopyridazino[4,5:2',3']pyrrolo[4',5'-d]pyridazine	61.48	2143	10.64	Alkaloid
5 1-Heptatriacotanol	63.16	2112	8.78	Fatty alcohol

Table 3 (cont'd). Volatile constituents of biochar obtained using POCV

Compound	RT (min)	RI <sup>(a)</sup>	% Peak Area	Functionality
6 17-Pentatriacontene	65.25	2300	14.33	Alkene
7 Ethyl iso-allocholate	65.77	2318	8.37	Alkaloid
8 octadecane, 3-ethyl-5-(2-ethylbutyl)-	68.18	2400	12.86	Alkane
9 1,3-benzenedicarboxylic acid, bis(2-ethylhexyl) ester	81.38	2844	21.01	Isophthalate

<sup>(a)</sup>Retention Index (HP 5ms column)

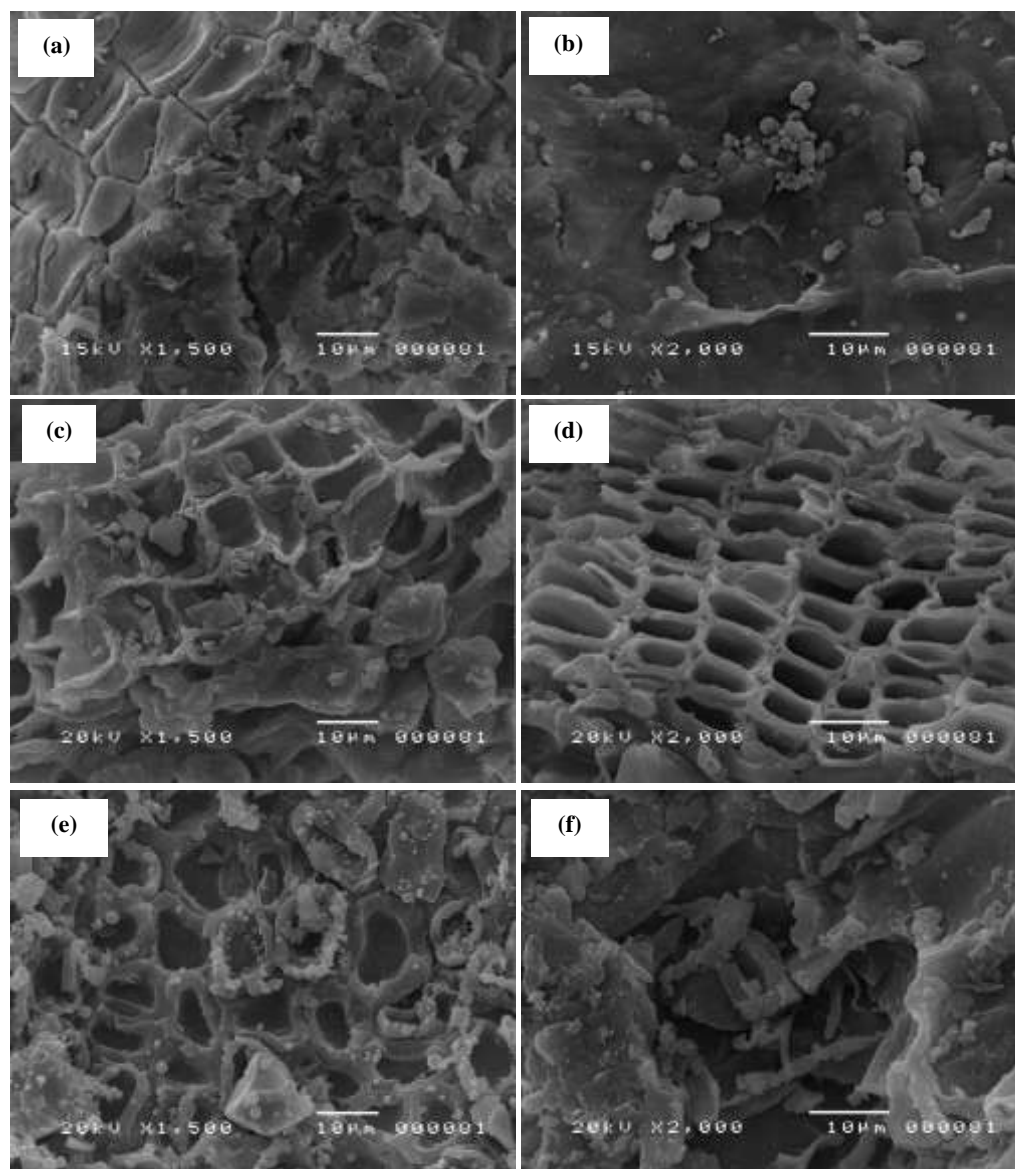


Figure 2. SEM images of MR bark (a-b), biochar product of *M. rubra* bark from HAR (c-d) and POCV (e-f)

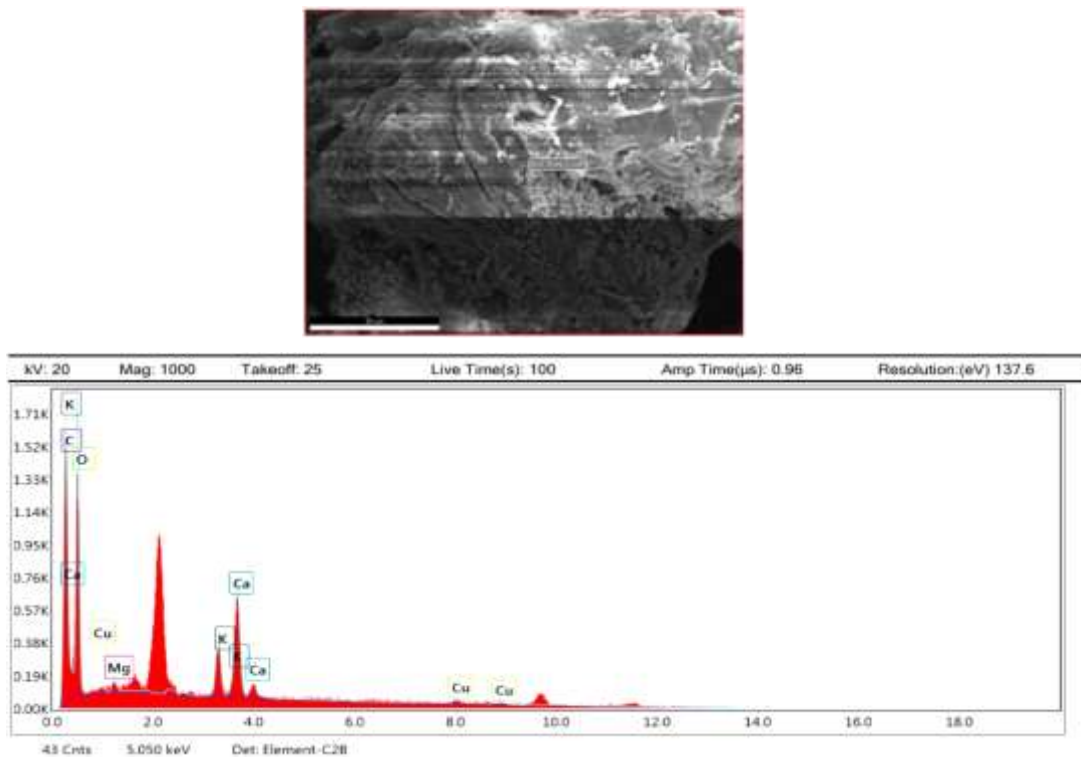


Figure 3. Image captured from the EDAX software and elemental analysis spectrum of dried bark of MR

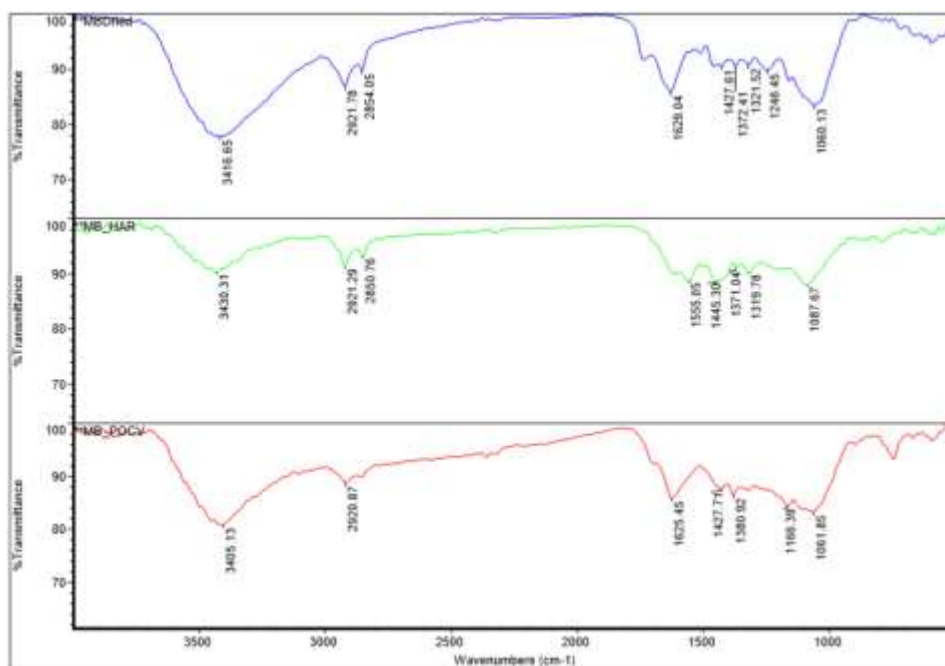


Figure 4. FTIR analysis of dried red mulberry bark (top) and biochars produced using HAR (middle) and POCV (bottom)

Table 4. IR absorptions of dried red mulberry bark

Wavenumber (cm <sup>-1</sup> )	Functional Group	Description
3416.65	O – H stretching	Alcohol
2921.78	C – H stretching	Alkane
2854.05	C – H stretching	Alkane
1629.04	C = C stretching	Conjugated alkene
1427.61	O – H bending	Carboxylic acid
1372.41	O – H bending	Phenol
1321.52	O – H bending	Phenol
1246.45	C – O stretching	Alkyl aryl ether
1060.13	C – O stretching	Primary alcohol

Table 5. IR absorptions of biochar of red mulberry bark produced from HAR

Wavenumber (cm <sup>-1</sup> )	Functional Group	Description
3430.31	O – H stretching	Alcohol
2921.29	C – H stretching	Alkane
2850.76	C – H stretching	Alkane
1555.05	C = C stretching	Cyclic alkene
1445.30	O – H bending	Carboxylic acid
1371.04	O – H bending	Phenol
1319.78	O – H bending	Phenol
1087.67	C – O stretching	Aliphatic ether

Table 6. IR absorptions of biochar of red mulberry bark produced from POCV

Wavenumber (cm <sup>-1</sup> )	Functional Group	Description
3405.13	O – H stretching	Alcohol
2920.87	C – H stretching	Alkane
1625.45	C = C stretching	Conjugated alkene
1427.71	O – H bending	Carboxylic acid
1380.92	C – H bending	Alkane
1166.39	C – O stretching	Tertiary alcohol
1061.85	C – O stretching	Primary alcohol

### Flame AAS analysis

Both biochars were analyzed for their ability to absorb heavy metals. After 72 hours, all samples under different test concentrations were analyzed using atomic absorption spectrophotometry. Results showed that both biochars absorbed lead (Pb) by more than 60%, with only 3.8 ppm of Pb remaining after incubating in 10 ppm of heavy metal solution (Table 7). On the other hand, the biochar samples absorbed only a minimal amount of cadmium (Cd) and iron (Fe) from the solution. Other heavy metals (Cr and Cu) were not effectively absorbed by both biochars.

Pb was absorbed the most among the metals tested in the prepared solution by both hydrochars derived from the bark of MR. Pb is considered as a highly poisonous environmental hazard affecting mostly plants. Moreover, Pb has been reported as second to the most hazardous substance, arsenic, with regards to frequency of occurrence, toxicity, and human exposure [44]. The oral lethal dose (LD) for humans is reported to be 714 mg/kg of lead acetate or about 450 mg/kg of Pb [45]. Pb can be easily bioremediated by different parts of the plant, although it is identified as a non-essential element. Excess lead can result to curbed growth, chlorosis, and darkening of the underground vascular network of the plant [46]. Mulberry plants are popularly cultivated as nourishment for silkworms in several nations [6]. One study reported the use of mulberry plant (*M. alba*) – silkworm system in a Pb-polluted soil detoxification process. The experiment revealed that the mulberry underground vascular systems of the plant adsorbed a significant amount of the Pb in the soil, where more than 90% of the Pb in the aerial parts built up in their cell walls [47].

Another study dedicated in the investigation of the absorbed metals in mulberry berries, *M. alba*, MR and *M. nigra*, was performed which revealed that Fe was highly accumulated, and that Cd was minimally accrued in all three mulberry fruits [48]. Cd is a non-essential element that may induce damage or toxicity to plants when accumulated which can cause stunted growth, chlorosis, and leaf rolls in plants [49]. White mulberry (*M. alba*) was reported to be suitable in phytoextracting

Cd and Ni. Different organs of *M. alba* were treated with varying levels of heavy metals such as Cd, Cr, and Ni. Green leaves were observed to contain higher amounts of Cd while fallen leaves had higher amounts of Cr and Ni compared to the roots and stem of white mulberry [14]. A dose of 0.5 mg/m<sup>3</sup> of Cd would result in respiratory distress from an 8-hour exposure, whereas a dose of 1-5 mg/m<sup>3</sup> of Cd is already reported as “immediately dangerous” for humans causing facial edema, hypotension, dysrhythmias, confusion and others [50]. In this study, the biochar samples absorbed nominal amounts of Cd and Fe from the heavy metal solution.

Fe is considered as a micronutrient for its minimal requirement for normal plant growth. Plants may suffer iron deficiency causing chlorosis and stunted growth. However, excessive intake of iron or iron overload may also induce toxicity. Fe toxicity has been one of the perceived problems affecting lowland rice plantation resulting in stunted growth and complete yield loss [51]. In humans, serum iron concentrations exceeding or equivalent to 350 µg/dl in 2- and 6-hours post-ingestion intervals suggested that serum iron content greater than 500 µg/dl would pose a dangerous hazard leading to acute liver malfunction [52]. In this study, minimal fluctuations in the content of Fe were observed in the heavy metal solution at 5 -10 ppm concentrations. However, at lower concentrations (0.5 - 1 ppm), both biochars absorbed most of Fe.

Unfortunately, Cr was not effectively absorbed by both biochars. This heavy metal is considered as a serious environmental pollutant which can induce toxicity and deleterious effects to plants including alterations in the germination process that can affect total dry matter and yield production [53]. Likewise, Cu concentration was not reduced significantly in the solutions.

Table 7. Total concentration of heavy metals absorbed by biochars of mulberry bark at different test concentrations after 72 hours of incubation

	Concentration (ppm)				
	Cd	Pb	Cr	Cu	Fe
HAR					
10 ppm	8.62 ± 0.01	3.84 ± 0.01	9.25 ± 0.03	9.76 ± 0.01	9.68 ± 0.01
5 ppm	*	4.27 ± 0.03	*	*	4.30 ± 0.02
1 ppm	*	*	*	*	0.33 ± 0.04
0.5 ppm	*	*	*	*	0.00 ± 0.00
POCV					
10 ppm	8.60 ± 0.04	3.74 ± 0.01	*	9.89 ± 0.02	9.99 ± 0.01
5 ppm	*	3.65 ± 0.01	*	*	4.65 ± 0.07
1 ppm	*	*	*	*	0.46 ± 0.10
0.5 ppm	*	*	*	*	0.00 ± 0.00

Data reported as mean ± standard deviation. \*no remediation observed

### Conclusion

Characterization of dried red mulberry bark (MR) revealed the presence of several phytosterols, triterpenes, triterpenoids, esters, alkanes, alkenes, alkaloids, diene, and fatty alcohols. POCV seemed to induce greater carbonization in biochars as reflected in the GC-EI-MS profile. Surface characterization of dried red mulberry bark and biochars revealed the presence of cork wood patterns typical in all woody plants, which are known to aid in the remediation process. Though the POCV samples displayed a less distinct pattern of cork wood in the SEM images compared to the regular patterns seen in HAR trials, both biochars of *M. rubra* L. bark effectively absorbed almost 60% of Pb in the heavy metal solution and minimal amounts of Cd and Fe. However, both biochars showed no effect in removing Cu and Cr in the solution. Based on the findings of this work, future research could be focused in the use of *M. rubra* biochar in water purification systems for both rural and commercial development, especially in areas where Pb contamination is evident.

### Acknowledgement

A research grant from De La Salle University Science Foundation, through the University Research Coordination Office, is gratefully acknowledged.

### References

1. Shaheen, S. M., Niazi, N. K., Hassan, N. E. E., Bibi, I., Wang, H., Tsang, D. C. W., Ok, Y. S., Bolan, N. and Rinklebe, J. (2019). Wood-based biochar for the removal of potentially toxic elements in water and wastewater: a critical review. *International Materials Reviews*, 64(4): 216-247.
2. Oni, B., Oziegbe, O. and Olawole, O. (2019). Significance of biochar application to the environment and economy. *Annals of Agricultural Sciences*, 64(2): 222-236.
3. Yang, X., Zhang, S., Ju, M. and Liu, L. (2019). Preparation and modification of biochar materials and their application in soil remediation. *Applied Sciences*, 9(7): 1365.

4. Vijayan, K., Tikader, A., Weiguo, Z., Nair, C., Ercisli, S. and Tsou, C. (2011). *Morus*. *Wild Crop Relatives: Genomic and Breeding Resources*: 75-95.
5. Jiang, Y., Huang, R., Yan, X., Jia, C., Jiang, S. and Long, T. (2017). Mulberry for environmental protection. *Pakistan Journal of Botany*, 49: 781-788.
6. Ercisli, S. and Orhan, E. (2007). Chemical composition of white (*Morus alba*), red (*Morus rubra*), and black (*Morus nigra*) mulberry fruits. *Food Chemistry*, 103: 1380-1384.
7. Sharma, S. B., Gupta, S., Ac, R., Singh, U. R., Rajpoot, R. and Shukla, S. K. (2010). Antidiabetogenic action of *Morus rubra* L. leaf extract in streptozotocin-induced diabetic rats. *Journal of Pharmacy and Pharmacology*, 62: 247-255.
8. Dhiman, S., Kumar, V., Mehta, C., Gat, Y. and Kaur, S. (2019). Bioactive compounds, health benefits and utilisation of *Morus* spp.– a comprehensive review. *The Journal of Horticultural Science and Biotechnology*, 95(1): 8-18.
9. Thabti, I., Elfalleh, W., Tlili, N., Ziadi, M., Campos, M. and Ferchichi, A. (2013). Phenols, flavonoids, and antioxidant and antibacterial activity of leaves and stem bark of *Morus* species. *International Journal of Food Properties*, 17(4): 842-854.
10. Demir, S., Turan, I., Aliyazicioglu, Y., Kilinc, K., Yaman, S. and Ayazoglu Demir, E. (2016). *Morus rubra* extract induces cell cycle arrest and apoptosis in human colon cancer cells through endoplasmic reticulum stress and telomerase. *Nutrition and Cancer*, 69(1): 74-83.
11. Selina, I. I. (2014). A comparative study of the amino acid composition of black mulberry (*Morus nigra* L.), white mulberry (*Morus alba* L.) and red mulberry (*Morus rubra* L.). *Basic Research*, 3(4): 770-774.
12. Ercisli, S., Tosun, M., Duralija, B., Voća, S., Sengul, M. and Turan, M. (2010). Phytochemical content of some black (*Morus nigra* L.) and purple (*Morus rubra* L.) mulberry genotypes. *Food Technology & Biotechnology*, 48(1): 102-106.
13. Nikolova, T. (2015). Absorption of Pb, Cu, Zn, and Cd type *Morus alba* L. cultivated on soils contaminated with heavy metals. *Bulgarian Journal of Agricultural Science*, 21(4): 747-750.
14. Rafati, M., Khorasani, N., Moattar, F., Shirvany, A., Moraghebi, F. and Hosseinzadeh, S. (2011). Phytoremediation potential of *Populus alba* and *Morus alba* for cadmium, chromium and nickel absorption from polluted soil. *International Journal of Environmental Research*, 5: 961-970.
15. Zama, E., Zhu, Y., Reid, B. and Sun, G. (2017). The role of biochar properties in influencing the sorption and desorption of Pb(II), Cd(II) and As(III) in aqueous solution. *Journal Of Cleaner Production*, 148: 127-136.
16. Biskup, E., Gołębiowski, M., Gniadecki, R., Stepnowski, P. and Łojkowska, E. (2012). Triterpenoid  $\alpha$ -amyirin stimulates proliferation of human keratinocytes but does not protect them against UVB damage. *Acta Biochimica Polonica*, 59(2): 255-260.
17. Santos, F., Frota, J., Arruda, B., de Melo, T., da Silva, A. and Brito, G. (2012). Antihyperglycemic and hypolipidemic effects of  $\alpha$ ,  $\beta$ -amyirin, a triterpenoid mixture from *Protium heptaphyllum* in mice. *Lipids in Health and Disease*, 11(1): 98.
18. Vázquez, LH., Palazon, J. and Navarro-Ocaña, A. (2012). The pentacyclic triterpenes  $\alpha$ ,  $\beta$ -amyirins: A review of sources and biological activities. In V. Rao (Ed), *Phytochemicals – A Global Perspective of Their Role in Nutrition and Health*. InTech: pp. 487-502.
19. Melo, C., Morais, T., Tomé, A., Brito, G., Chaves, M., Rao, V. and Santos, F. (2011). Anti-inflammatory effect of  $\alpha$ ,  $\beta$ -amyirin, a triterpene from *Protium heptaphyllum*, on cerulein-induced acute pancreatitis in mice. *Inflammation Research*, 60(7): 673-681.
20. Victor, M., David, J., dos Santos, M., Barreiros, A., Barreiros, M. and Andrade, F. (2017). Synthesis and evaluation of cytotoxic effects of amino-ester derivatives of natural  $\alpha$ ,  $\beta$ -amyirin mixture. *Journal of The Brazilian Chemical Society*, 28(11): 2155-2162.

21. National Center for Biotechnology Information. PubChem Database. Lanosterol, CID=246983, <https://pubchem.ncbi.nlm.nih.gov/compound/Lanosterol> [Access online 10 July 2020].
22. Zhao, L., Chen, X., Zhu, J., Xi, Y., Yang, X. and Hu, L. (2015). Lanosterol reverses protein aggregation in cataracts. *Nature*, 523(7562): 607-611.
23. Daszynski, D., Santhoshkumar, P., Phadte, A., Sharma, K., Zhong, H., Lou, M. and Kador, P. (2019). Failure of oxysterols such as lanosterol to restore lens clarity from cataracts. *Scientific Reports*, 9(1): 8459.
24. Shanmugam, P., Barigali, A., Kadaskar, J., Borgohain, S., Mishra, D., Ramanjulu, R. and Minija, C. (2015). Effect of lanosterol on human cataract nucleus. *Indian Journal of Ophthalmology*, 63 (12): 888.
25. Tripathi, N., Kumar, S., Singh, R., Singh, C., Singh, P. and Varshney, V. (2013). Isolation and identification of  $\gamma$ -sitosterol by GC-MS from the leaves of *Girardinia heterophylla* (Decne). *The Open Bioactive Compounds Journal*, 4(1): 25-27.
26. Endrini, S., Rahmat, A., Ismail, P. and Taufiq-Yap, Y. (2015). Cytotoxic effect of  $\gamma$ -sitosterol from Kejibeling (*Strobilanthes crispus*) and its mechanism of action towards *c-myc* gene expression and apoptotic pathway. *Medical Journal of Indonesia*, 23(4): 203-208.
27. Corey, E., Hess, H. and Proskow, S. (1963). Synthesis of a  $\beta$ -amyrin derivative, olean-11,12;13,18-diene. *Journal of The American Chemical Society*, 85(24): 3979-3983.
28. de Almeida, P., Boleti, A., Rüdiger, A., Lourenço, G., da Veiga Junior, V. and Lima, E. (2015). Anti-inflammatory activity of triterpenes isolated from *Protium paniculatum* oil-resins. *Evidence-Based Complementary and Alternative Medicine*, 2015: 1-10.
29. Belakhdar, G., Benjouad, A. and Abdennebi, E.H. (2015). Determination of some bioactive chemical constituents from *Thesium humile* vahl. *Journal of Materials and Environmental Science*, 6(10): 2778-2783.
30. Quarta, A., Novais, R., Bettini, S., Iafisco, M., Pullar, R. and Piccirillo, C. (2019). A sustainable multi-function biomorphic material for pollution remediation or UV absorption: Aerosol assisted preparation of highly porous ZnO-based materials from cork templates. *Journal of Environmental Chemical Engineering*, 7(2): 102936.
31. Yashvanth, S., Shobha Rani, S. and Madhavendra, SS. (2015). *Morus alba* L., A New Perspective: Scan-ning electron microscopic, micro chemical, GC-MS and UPLC-MS characterisation. *International Journal of Research in Pharmacy and Chemistry*, 5(1): 106-115.
32. InfoPlease (2020). Carbon (element): Biological importance. Access from <https://www.infoplease.com/encyclopedia/science/chemistry/elements/carbon/biological-importance>. [Access online 13 July 2020].
33. Chantuma, P., Lacoite, A., Kasemsap, P., Thanisawanyangkura, S., Gohet, E. and Clement, A. (2009). Carbohydrate storage in wood and bark of rubber trees submitted to different level of C demand induced by latex tapping. *Tree Physiology*, 29(8): 1021-1031.
34. Krutul, D., Zielenkiewicz, T., Radomski, A., Zawadzki, J., Antczak, A., Drożdżek, M. and Makowski, T. (2011). Metals accumulation in scots pine (*Pinus sylvestris* L.) wood and bark affected with environmental pollution. *Wood Research*, 2017(62): 353-364.
35. Ross, A., Taylor, C., Yaktine, A. and Cook, H. (2011). Dietary reference intakes for calcium and vitamin D. The National Academies Press, Washington, DC.
36. Haas, E. (2011). Role of potassium in maintaining health. Access from <https://hkpp.org/patients/potassium-health> [Access online 13 July 2020].
37. National Academies of Sciences, Engineering, and Medicine (2019). Dietary reference intakes for sodium and potassium. The National Academies Press, Washington, DC.
38. Schwalfenberg, G. and Genuis, S. (2017). The importance of magnesium in clinical healthcare. *Scientifica*, 2017: 1-14.



39. Institute of Medicine (1997). Dietary reference intakes: Calcium, phosphorus, magnesium, vitamin D and fluoride. National Academy Press, Washington, DC.
40. Institute of Medicine Panel (US) on Micronutrients (2001). Dietary reference intakes for vitamin A, vitamin K, arsenic, boron, chromium, copper, iodine, iron, manganese, molybdenum, nickel, silicon, vanadium, and zinc. The National Academies Press, Washington, DC.
41. National Research Council (US) Committee on Copper in Drinking Water (2000). Copper in drinking water. National Academy Press, Washington, DC.
42. Jose, J. C., Oyong, G., Ajero, M. D., Chiong, I., Cabrera, E., Tan, M. C. S. (2020). Insights on the chemical constituents and hydrothermal carbonization of *Crescentia cujete* L.. *Malaysian Journal of Analytical Sciences*, 24(1): 134-145.
43. Naron, D., Collard, F., Tyhoda, L. and Görgens, J. (2019). Production of phenols from pyrolysis of sugarcane bagasse lignin: Catalyst screening using thermogravimetric analysis – thermal desorption – gas chromatography – mass spectroscopy. *Journal of Analytical and Applied Pyrolysis*, 138: 120-131.
44. Pourrut, B., Shahid, M., Dumat, C., Winterton, P. and Pinelli, E. (2011). Lead uptake, toxicity, and detoxification in plants. *Reviews of Environmental Contamination and Toxicology*, 213:113-136.
45. Centers for Disease Control and Prevention (2020). CDC - immediately dangerous to life or health concentrations (IDLH): Lead compounds (as Pb) - NIOSH publications and products. Access from <https://www.cdc.gov/niosh/idlh/7439921.html>. [Accessed online 16 July 2020].
46. Sharma, P. and Dubey, R. S. (2005). Lead toxicity in plants. *Brazilian Journal of Plant Physiology*, 17(1): 35-52.
47. Zhou, L., Zhao, Y., Wang, S., Han, S. and Liu, J. (2015). Lead in the soil–mulberry (*Morus alba* L.)–silkworm (*Bombyx mori*) food chain: Translocation and detoxification. *Chemosphere*, 128: 171-177.
48. Micić, R., Dimitrijević, D., Kostić, D., Stojanović, G., Mitić, S. and Mitić, M. (2013). Content of heavy metals in mulberry fruits and their extracts–correlation analysis. *American Journal of Analytical Chemistry*, 4(11): 674-682.
49. Benavides, M. P., Gallego, S. M. and Tomaro, M. L. (2005). Cadmium toxicity in plants. *Brazilian Journal of Plant Physiology*, 17(1): 21-34.
50. Bull, S. (2010). Cadmium toxicological overview. Access from [https://assets.publishing.service.gov.uk/government/uploads/system/uploads/attachment\\_data/file/337542/hpa\\_cadmium\\_toxicological\\_overview\\_v3.pdf](https://assets.publishing.service.gov.uk/government/uploads/system/uploads/attachment_data/file/337542/hpa_cadmium_toxicological_overview_v3.pdf). [Accessed online 16 July 2020].
51. Baruah, K. K. and Bharali, A. (2015). Physiological basis of iron toxicity and its management in crops. In: Amrit L.S. Recent advances in crop physiology. Daya Publishing House®, New Delhi, India
52. Abhilash, K., Arul, J. and Bala, D. (2013). Fatal overdose of iron tablets in adults. *Indian Journal of Critical Care Medicine*, 17(5): 311-313.
53. Shanker, A., Cervantes, C., Lozavera, H. and Avudainayagam, S. (2005). Chromium toxicity in plants. *Environment International*, 31(5): 739-753.